Published in final edited form as:
Free Radic Biol Med. 2013 October ; 63: 390–398. doi:10.1016/j.freeradbiomed.2013.05.030.

High Fat Diet Induces Changes in Adipose Tissue *trans*-4-Oxo-2-Nonenal and *trans*-4-Hydroxy-2-Nonenal Levels in a Depot-Specific Manner

Eric K. Long[1], **Dalay M. Olson**[1,2], and **David A. Bernlohr**[1,3]

[1]Department of Biochemistry, Molecular Biology, and Biophysics, University of Minnesota, Minneapolis, MN 55455

[2]Graduate Program of Integrative Biology and Physiology, University of Minnesota, Minneapolis, MN 55455

Abstract

Protein carbonylation is the covalent modification of proteins by α,β-unsaturated aldehydes produced by non-enzymatic lipid peroxidation of polyunsaturated fatty acids. The most widely studied aldehyde product of lipid peroxidation, *trans*-4-hydroxy-2-nonenal (4-HNE), is associated with obesity-induced metabolic dysfunction and has demonstrated reactivity toward key proteins involved in cellular function. However, 4-HNE is only one of many lipid peroxidation products and the lipid aldehyde profile in adipose tissue has not been characterized. To further understand the role of oxidative stress in obesity-induced metabolic dysfunction, a novel LC-MS/MS method was developed to evaluate aldehyde products of lipid peroxidation and applied to the analysis of adipose tissue. 4-HNE and *trans*-4-oxo-2-nonenal (4-ONE) were the most abundant aldehydes present in adipose tissue. In high fat fed C57Bl/6J and *ob/ob* mice the levels of lipid peroxidation products were increased 5–11 fold in epididymal adipose, unchanged in brown adipose but decreased in subcutaneous adipose tissue. Epididymal adipose tissue of high fat fed mice also exhibited increased levels of proteins modified by 4-HNE and 4-ONE while subcutaneous adipose tissue levels of these modifications were decreased. High fat feeding of C57Bl/6J mice resulted in decreased expression of a number of genes linked to antioxidant biology selectively in epididymal adipose tissue. Moreover, TNFα treatment of 3T3-L1 adipocytes resulted in decreased expression of GSTA4, GPx4, and Prdx3 while up regulating the expression of SOD2. These results suggest that inflammatory cytokines selectively down regulate antioxidant gene expression in visceral adipose tissue resulting in elevated lipid aldehydes and increased protein carbonylation.

Keywords

adipose; obesity; oxidative stress; 4-HNE; 4-ONE; gene expression

[3]Author to whom correspondence should be addressed David A. Bernlohr Department of Biochemistry, Molecular Biology and Biophysics The University of Minnesota 321 Church St. SE Minneapolis, MN 55455 bernl001@umn.edu 1.612.624.2712.

INTRODUCTION

Obesity is characterized by increased adiposity and frequently results in the development of insulin resistance and type 2 diabetes [1–3]. Obesity-induced insulin resistance is accompanied by a number of molecular changes in adipose tissue [4–7] including increased macrophage infiltration, particularly in the visceral depots, increased ER stress and mitochondrial dysfunction [8, 9]. Of particular interest is increased oxidative stress that results in elevated protein carbonylation that occurs coincident with the development of insulin resistance [4, 5, 10–13]. Given the importance of cysteine, lysine and histidine (protein carbonylation targets) in catalysis, proteins modified by reactive aldehydes are typically inactivated and may be targeted for degradation. However, some signaling systems are activated upon carbonylation [13–17]. Protein carbonylation is believed to play a major role in altering mitochondrial respiration and metabolic capacity [4, 18, 19] and recently Curtis et al., have identified the mitochondrial phosphate carrier and two subunits of Complex I (NDUFA2 and NDUFA3) as critical carbonylation targets using the 3T3-L1 model cell system [10].

Reactive α,β-unsaturated aldehydes responsible for protein carbonylation are products of lipid peroxidation that result from oxidative modification of polyunsaturated fatty acids (PUFA) [20]. These α,β-unsaturated aldehydes are believed to play a major role in onset and progression of disease [15]. *Trans*-4-hydroxy-2-nonenal (4-HNE) is the most widely studied α,β-unsaturated aldehyde. 4-HNE is moderately reactive and freely diffuses within the cell and across membranes [13, 21, 22]. A number of studies have demonstrated that 4-HNE is cytotoxic, depletes glutathione, induces mitochondrial dysfunction, and targets some enzymes for degradation in a number of cell culture systems [6, 14, 19, 23]. In addition, 4-HNE has been linked to obesity-induced insulin resistance [7, 24].

While 4-HNE has received a great deal of attention, a number of other α,β-unsaturated aldehydes result from lipid peroxidation [25]. The aldehyde profile resulting from lipid peroxidation depends on the PUFA composition of the tissue in question. As such, the cellular consequences of lipid peroxidation depend largely on the profile of aldehydes produced, as they vary to a great degree in rates of formation and metabolism, diffusibility, and reactivity. For example, *In vitro* studies have shown that lipid peroxidation of linoleic acid, the most abundant PUFA in adipose tissue, results primarily in production of 4-HNE and *trans*-4-oxo-2-nonenal (4-ONE), suggesting that 4-ONE may be an important effector of oxidative stress in adipose tissue [26].

A variety of Phase I and Phase II antioxidant enzymes have been implicated in enzymatic detoxification of reactive lipid aldehydes [5]. Aldehyde dehydrogenase has been considered a key antioxidant enzyme catalyzing the oxidation of aldehydes to the corresponding carboxylic acid and in addition a variety of glutathione peroxidases and peroxiredoxins have been suggested to play major roles in lipid hydroperoxide reduction, preventing formation of lipid aldehydes [27–29]. The key Phase II enzyme responsible for Michael adduction of lipid aldehydes is to glutathione is glutathione S-transferase A4 and mice lacking GSTA4 exhibit increased protein carbonylation and metabolic dysfunction [10].

Despite numerous studies showing increases in protein carbonylation and mitochondrial dysfunction as a result of diet-induced obesity, the specific aldehydes responsible for these processes have not been identified [4, 5, 10–12]. To this end, a novel method was developed and validated for quantitation of individual aldehydes in adipose tissue of high fat-fed C57Bl/6J or *ob/ob* mice. We report herein that high fat fed and *ob/ob* mice exhibited increased levels of 4-HNE and 4-ONE in epididymal white adipose tissue (EWAT). In contrast, feeding a high fat diet resulted in significant decreases in subcutaneous white

adipose tissue (SAT) 4-HNE and 4-ONE content without any alteration in aldehyde content of brown adipose tissue. Consistent with these results, 4-HNE/4-ONE Michael adducts were increased in EWAT of high fat-fed mice, but decreased in SAT of high fat-fed mice. Furthermore, EWAT of *ob/ob* and high fat-fed mice displayed general decreases in expression of genes encoding key metabolic enzymes while expression of these enzymes remained relatively unaltered in SAT of *ob/ob* and high fat-fed mice.

MATERIALS AND METHODS

Materials

4-HNE, 4-ONE, *trans*-4-hydroxy-2-hexenal (4-HHE), *trans*-4-hydroxy-2-nonenal-9,9,9-d_3 (4-HNE-d_3), and *trans*-4-oxo-2-nonenal-9,9,9-d_3 (4-ONE-d_3) were purchased from Cayman Chemical (Ann Arbor, MI). *Trans*-2-octenal, and butylated hydroxytoluene (BHT) were purchased from Sigma-Aldrich (St. Louis, MO). Acrolein, *trans*-2-butenal, and carboxymethoxylamine (aminooxyacetic acid, AOA) were purchased from Acros Organics (Geel, Belgium). Diethylenetriaminepentaacetic acid (DTPA) was purchased from TCI America (Portland, OR). Malondialdehyde (MDA) was synthesized as previously published [25, 30]. High fat diet containing 60% of calories from lard was purchased from BioServ (Frenchtown, NJ). Strata-X-AW weak anion exchange solid phase extraction columns were purchased from Phenomenex (Torrance, CA). 10 week old *ob/ob* leptin deficient mice were purchased from Jackson Laboratories (Bar Harbor, ME). Anti-HNE Michael adduct polyclonal primary antibody was purchased from Calbiochem (No. 393207), a subsidiary of EMD Millipore (Billerica, MA). Goat polyclonal anti-actin (No. sc-1616) was purchased from Santa Cruz Biotechiology (Santa Cruz, CA). Horseradish peroxidase-linked rabbit anti-goat IgG antibody (No. NB710-H) was purchased from Novus Biologicals (Littleton, CO). Restore Plus Western Blot Stripping Buffer (No. 46430), SuperBlock Blocking Buffer (No. 37536), and SuperSignal West Pico Chemiluminescent Substrate (No. 34087) were purchased from Thermo Scientific (Rockford, IL).

Differentiation of 3T3-L1 adipocytes and cytokine treatment

3T3-L1 fibroblasts grown to confluence and differentiated using the standard dexamethasone, methylisobutylxanthine and insulin protocol [31]. Differentiation was assessed by triglyceride accumulation and the expression of adipocyte marker proteins such as the adipocyte fatty acid binding protein, hormone sensitive lipase and the insulin-stimulatable glucose transporter. On day 8 of differentiation cells were treated with 1nmol/L TNFα (R&D systems, Minneapolis) for 24 hours and subsequently harvested for RNA analysis.

Animal Protocol

Wild-type C57Bl/6J mice were weaned and maintained on either a high fat (20% protein, 35.5% fat, 36.3% carbohydrate; Bioserv, Frenchtown, NJ) or chow diet at 3 weeks of age. Ob/ob mice were purchased at 10 weeks of age and maintained for 2 weeks on normal chow diet prior to sacrifice. At 12 weeks of age (9 weeks on diet for high fat and chow fed controls), animals were sacrificed and selected tissues were removed and flash frozen in liquid nitrogen. Frozen tissues were stored at −80° C prior to analysis. All samples were prepared for analysis less than 1 month after dissection and storage. The University of Minnesota Institutional Animal Care and Use Committee approved all animal procedures.

Derivatization of Aldehydes and Solid Phase Extraction

100 mg of adipose tissue was homogenized in 50 mM sodium acetate buffer containing 5 mM aminooxyacetic acid with 250 μM BHT and 500 μM DTPA at pH 5.0, spiked with

deuterated internal standards, and incubated for 1h on ice. Derivatization resulted in oxime formation as shown in Figure 1. After derivatization, samples were vortexed briefly and centrifuged at 10,000g for 10 minutes. Strata-X-AW columns (60 mg sorbent) were conditioned with 1 mL methanol and equilibrated with 1 mL 100 mM sodium acetate, pH 5.3. The aqueous phase of samples was loaded and columns were washed with 1 mL 100 mM sodium acetate buffer, pH 5.3 followed by 1 mL methanol. Columns were dried briefly under vacuum, and derivatized aldehydes were eluted with 1 mL 5:95 NH_4OH:MeOH. Eluates were dried to a film under nitrogen, resuspended in 125 μL MeOH and stored at −80° C prior to analysis by LC-MS/MS. Immediately preceding LC-MS/MS analysis, samples were diluted to 250 μL with water in order to bring the concentration of aldehyde derivatives in the sample within the linear range validated for analysis.

Liquid Chromatography-Tandem Mass Spectrometry

LC-MS/MS was carried out on an Agilent 1100 HPLC coupled to an AB/Sciex API 4000Qtrap mass spectrometer. Chromatography was performed using a 100 mm × 2.1 mm Agilent Zorbax Eclipse plus C18 column with a 3.5 micron particle size using a gradient elution. Solvent A was 0.1% formic acid in water and Solvent B was acetonitrile containing 0.1% formic acid. The column was equilibrated at 95:5 A:B. After sample injection, the mobile phase was held at 95:5 for 3 minutes after which time solvent B was increased to 100% using a linear gradient from 3–15 minutes. Solvent B was held at 100% for 3 minutes, followed by equilibration at 95% solvent A. A representative chromatogram of synthetic standards is depicted in Figure 2.

Multiple reaction monitoring (MRM) conditions were developed using direct infusion tandem mass spectrometry. MRM transitions are listed in Table 1. Analyses were performed using electrospray ionization with an ionspray voltage of −4500V. Collision energy for all analytes was −15V, with the exception of malondialdehyde (−10V). Stable isotope dilution was used for quantitation of aldehydes in tissue samples and final quantities were normalized by weight of tissue homogenized. Values are presented as nanograms of aldehyde per gram of tissue.

Adipose Tissue Aldehyde Screening

100 mg of EWAT was prepared and analyzed for eight potential products of lipid peroxidation: malondialdehyde, acrolein, *trans*-2-butenal, 4-HHE, *trans*-2-hexenal, 4-HNE, 4-ONE, and *trans*-2-octenal. 4-HNE, 4-ONE, and MDA were detectable in all samples, with *trans*-2-octenal present at low levels in some samples. The abundance of 4-HNE was similar to that of 4-ONE but much greater than MDA, The absolute levels of 4-HNE and 4-ONE were ~300–500 ng/g tissue while MDA was present at ~20 ng/g tissue (data not shown). Based on abundance and far greater reactivity of 4-HNE and 4-ONE as compared to MDA and *trans*-2-octenal, validation parameters were acquired for 4-ONE and 4-HNE.

Method Validation Parameters

50 mg of tissue homogenate was spiked with varying concentrations of 4-ONE and 4-HNE with a constant amount of 4-HNE-d_3 and 4-ONE-d_3. Endogenous levels of 4-HNE and 4-ONE were determined in quadruplicate in homogenate spiked only with deuterated internal standards, and subtracted from each sample. The linear range of this assay was 20 fmol to at least 1000 fmol for both 4-HNE and 4-ONE (Figure 3). Intra-day precision was assayed at six concentrations (10, 20, 50, 100, 250, and 1000 fmol) in quadruplicate. Precision, as determined by percent relative standard deviation (%RSD), was within the acceptable range (<20%) from 20 –1000 fmol (Table 2). Accuracy was determined at four concentrations (20, 50, 250, and 1000 fmol) in quadruplicate and was within the acceptable range at 50, 250, and 1000 fmol, but not at 20 fmol (Table 3). Based on the results of these validation

parameters, lower limit of quantitation was defined as 50 fmol based on acceptable values for accuracy, precision and linearity [32].

Measurement of 4-HNE/4-ONE Protein Adducts

250 mg of EWAT or SAT was homogenized in pH 5.5 sodium acetate buffer containing 250 μM BHT using an electronic homogenizer. Samples were vortexed briefly and centrifuged at 3800 rpm for 10 minutes at 4° C. The protein concentration was determined by the bicinchoninic acid protein quantitation assay (Sigma-Aldrich, St. Louis, MO). EWAT samples (20 μg of protein per sample) were separated by sodium dodecyl sulfate-polyacrylamide gel electrophoresis on a 12–20% gradient polyacrylamide gel, while SAT samples were separated on a 10% polyacrylamide gel. After separation, proteins were transferred to Immobilon-FL membranes (Millipore, Darmstadt, Germany) and reduced for 1h with 50 mM sodium borohydride in phosphate-buffered saline (PBS). Membranes were then blocked using LI-COR Odyssey Imaging Systems (LI-COR Biosciences, Lincoln, NE) blocking buffer for 45 minutes prior to overnight incubation at 4° C with the anti-4-HNE/4-ONE Michael adduct antibody. Membranes were washed 4 times with PBS containing 0.2% Tween-20 (PBS-T), then incubated with LI-COR goat anti-rabbit IR-800 secondary antibody for 1h at room temperature. Membranes were washed 4 times with PBS-T and visualized using a LI-COR Odyssey imaging system.

For normalization, membranes were stripped with Restore Plus western blot stripping buffer for 7 minutes. Membranes were washed 4X with PBS-T and blocked with Superblock blocking buffer for 30 minutes prior to overnight incubation at 4° C with 1:1000 goat polyclonal anti-actin antibody. Membranes were washed 4X with PBS-T, then incubated for 1h with 1:50,000 HRP-linked rabbit anti-goat polyclonal antibody. Membranes were washed 4X with PBS-T and incubated with HRP substrate for 5 minutes. Bands were detected by autoradiography.

Quantitative Real Time PCR (qPCR)

Total RNA was extracted from 3T3-L1 cells and tissue using TRIzol reagent according to manufacturer's protocol (Invitrogen, Grand Island, NY). Both subcutaneous and epidiymal adipose tissue were harvested from age matched lean, ob/ob and high fat fed mice. Real-time amplification was performed using a Bio-Rad MyiQ thermocycler using iQ SYBR Green Supermix and recommended thermocycler parameters (Bio-Rad, Hercules, CA). Gene expression assays were performed for glutathione peroxidase 4 (Gpx4), peroxiredoxin 3 (Prdx3), manganese superoxide dismutase (SOD2), glutathione-S-transferase A4 (GSTA4), and aldehyde dehydrogenase 2 (ALDH2) (Primer sets shown in Table 4). Relative gene expression comparisons were carried out using transcription factor 2E (TFIIE) as an endogenous control.

Statistical Analyses

All statistical analyses were done using unpaired two-tailed student's t-tests with significance level set at $p<0.05$.

RESULTS

Quantitation of 4-HNE and 4-ONE in Adipose Tissue

To evaluate the levels of aldehydes in adipose tissue, high fat fed and chow fed C57Bl/6J and *ob/ob* mice were sacrificed and EWAT and SAT adipose depots harvested. Samples were homogenized, derivatized with aminooxyacetic acid and analyzed via liquid chromatography tandem mass spectrometry. In EWAT, levels of 4-HNE were increased >5-fold in high fat fed (HF) C57Bl/6J and chow fed ob/ob mice as compared to chow fed

controls (LF) ($p<0.05$) (Figure 4A). Similarly, 4-ONE levels were significantly increased >10-fold in adipose tissue of high fat fed C57Bl/6J and ob/ob mice as compared to chow fed controls ($p<0.05$) (Figure 4A). In contrast, 4-HNE and 4-ONE were significantly decreased in SAT of high fat fed versus chow fed mice (Figure 4B). 4-ONE and 4-HNE were not significantly decreased in SAT of *ob/ob* mice, although levels were reduced to approximately 50% of control levels (Figure 4B). 4-ONE and 4-HNE levels did not differ in brown adipose tissue as a result of high fat diet (Figure 4C).

4-HNE/4-ONE Protein Adduct Analysis

Given the changes in reactive aldehydes in the various adipose depots we assessed the levels of protein carbonylation in the various adipose depots of high fat fed mice compared to chow fed controls using an antibody directed towards 4-HNE/4-ONE protein Michael adducts. Due to the reduction step used in this assay, 4-ONE and 4-HNE protein adducts are both reduced to 1,4-dihydroxynonene adducts and are indistinguishable [33]. Similar to the increased aldehydes in EWAT, high fat-fed mice exhibited increased levels of 4-HNE/4-ONE protein adducts compared to chow fed mice (Figure 5A). These results agree with previous reports that protein carbonylation is increased in EWAT in response to high fat diet [4, 11]. In contrast, 4-HNE/4-ONE Michael adducts were significantly decreased in SAT in high fat-fed mice as compared to chow fed mice (Figure 5B). These results are consistent with the observation that 4-HNE and 4-ONE levels are decreased in SAT of high fat-fed and *ob/ob* mice.

Expression Levels of Antioxidant Genes in Adipose Tissue

Because lipid aldehydes are formed via hydroxyl radical mediated oxidation of polyunsaturated fatty acyls that are regulated by a series of antioxidant enzymes, epididymal and subcutaneous adipose tissue of chow and high fat fed C57Bl/6J and *ob/ob* mice were analyzed for expression of a panel of antioxidant genes using quantitative real time PCR. Adipose tissue from high fat fed and *ob/ob* mice exhibited significantly decreased expression of GSTA4 and Prdx3 in EWAT. EWAT from high fat fed mice showed significantly decreased expression of Gpx4 (Figure 6A) and Gpx3 (results not shown). Interestingly, the level of GPx1 did not change in response to high fat feeding (results not shown). SOD2 expression did not change significantly as a result of high fat diet, but was significantly increased in EWAT of *ob/ob* mice (Figures 6A, C). ALDH2 and Gpx4 expression levels were significantly decreased in EWAT while they showed no change in expression in SAT of high fat fed as compared to chow fed mice (Figures 6A, B). However, ALDH2 expression was decreased in both EWAT and SAT while Gpx4 expression levels remained unchanged in ob/ob mice as compared to wild-type controls (Figures 6C, D). In subcutaneous adipose tissue, GSTA4 expression was significantly decreased in *ob/ob* mice with a trend toward decreased expression in high fat fed mice, consistent with previous studies (Figures 6B, D). In contrast to EWAT, Prdx3, Gpx4 and Gpx3 (data not shown) expression did not change significantly in SAT of high fat fed and ob/ob mice (Figures 6B, D). However, Gpx4 showed a trend toward increased expression in SAT of ob/ob mice (Figure 6D). SOD2 expression was not significantly changed in SAT of either high fat fed or *ob/ob* mice (Figures 6B, D).

Since visceral adipose depots are known to be infiltrated with inflammatory macrophages preferentially compared to subcutaneous depots we assessed the effect of inflammatory cytokines on antioxidant gene expression using the 3T3-L1 cell culture system. Figure 7 demonstrates that treatment of 3T3-L1 adipocytes with 1nM of TNFα for 24 h led to the down regulation of GSTA4, Prdx3, GPx4 while increasing the expression of SOD2. As such, a plausible mechanistic basis for the decreased expression of antioxidant genes in EWAT inflammatory cytokine-mediated down regulation.

DISCUSSION

Obesity-induced insulin resistance and resultant type 2 diabetes is strongly linked to oxidative stress and mitochondrial dysfunction [4, 5, 10–12, 24]. Also associated with obesity is a state of chronic low-grade inflammation characterized by increased macrophage infiltration to adipose tissue and resultant increases in pro-inflammatory cytokines such as TNF-α, IL-6 and IL-1β [8, 34, 35]. In studies of insulin resistance, protein carbonylation is often used as a biomarker of oxidative stress in adipose and other tissues and correlates positively with metabolic dysfunction [4, 5, 10–12, 24]. While immunodetection of protein carbonylation provides information regarding total oxidative state of the tissue, it does not provide specific information as to the composition of aldehydes responsible for modification but have largely been assumed to be due to 4-HNE [15, 36–38]. The effects of 4-HNE on cellular systems and the correlation between 4-HNE modifications of proteins and disease have been well defined [6, 17, 23, 36, 39–49].

In adipose tissue, linoleic acid is the most abundant PUFA, representing 15–40 mole-percent of total fatty acid [50, 51]. Based on these levels, it is very likely that lipid peroxidation products of linoleic acid are the driving force behind oxidative stress-induced protein carbonylation. Indeed, one study suggests that 4-substituted alkenals are major products of lipid peroxidation in adipose tissue of mice fed a high fat diet as determined by derivatization and colorimetric analysis [6]. The results were attributed to 4-HNE despite the inability of this method to distinguish distinct 4-substituted alkenals [52]. As 4-ONE is a major lipid peroxidation product of linoleic acid, it is possible that the results obtained via this method represent 4-ONE, or a mixture of 4-HNE and 4-ONE [26].

Application of a novel LC-MS/MS method confirmed the hypothesis that 4-HNE and 4-ONE are the major products of lipid peroxidation in adipose tissue, and that both increase in abundance in EWAT of high fat fed or *ob/ob* mice. While obesity-induced increases in oxidative stress and lipid peroxidation are widely accepted, the finding that 4-ONE is abundant in adipose tissue is a novel observation. Reactive oxygen species production occurs largely in mitochondria [53] and radicals responsible for peroxidation of PUFA are short-lived, this process likely occurs in mitochondrial membranes and in triglyceride droplets closely neighboring mitochondria. These spatial considerations are important in that mitochondrial protein carbonylation is increased in visceral adipose tissue in response to over nutrition, and isolated mitochondria of animals fed high fat diet display considerable alterations in mitochondrial respiration [4, 10]. As 4-ONE is >100-fold more reactive than 4-HNE, 4-ONE may selectively modify mitochondrial proteins and act as a major effector of oxidative stress-induced mitochondrial dysfunction [21, 22]. Interestingly, RAW 264.7 and primary peritoneal macrophages did not produce detectable levels of 4-HNE or 4-ONE (data not shown). In contrast, primary adipocytes and 3T3-L1 adipocytes did produce both 4-HNE and 4-ONE (data not shown) suggesting that adipocytes may be the primary producers of lipid aldehydes in adipose tissue.

Consistent with the reactivity differences between 4-ONE and 4-HNE, a recent report by Picklo et al. showed that 4-ONE is a more potent inducer of mitochondrial uncoupling (IC_{50} = 5μM) than 4-HNE (IC_{50} > 100μM) [18]. Assuming aldehydes are diffusible within the entire adipocyte, the concentration of 4-HNE and 4-ONE in adipose tissue is estimated to be ~2–5 μM. This estimate suggests that 4-ONE is present at concentrations sufficient to induce mitochondrial uncoupling while 4-HNE levels are ~20–50 fold lower than the IC_{50} for mitochondrial uncoupling.

Previous studies have documented changes in antioxidant gene expression in visceral and subcutaneous adipose tissue depots individually, but direct comparisons are sparse [57, 58].

The results of RT-PCR analysis showed that GSTA4, ALDH2 and Prdx3 gene expression decreased significantly in EWAT of high fat fed C57Bl/6J and *ob/ob* mice compared to chow fed mice. GSTA4 is the primary glutathione-S-transferase responsible for glutathionylation of 4-HNE and 4-ONE, and is known to be significantly down regulated with obesity [12]. This down regulation directly contributes to increased levels of 4-HNE and 4-ONE by reducing metabolic capacity [59–61]. In addition, decreased GPx4 and Prdx3 in EWAT of high fat fed mice are linked to decreased hydrogen peroxide and lipid hydroperoxide metabolism allowing for greater production 4-HNE and 4-ONE [62, 63]. Specifically, hydrogen peroxide accumulation provides substrate for Fenton chemistry-mediated production of hydroxyl radical, which induces lipid peroxidation. In conjunction, decreased lipid hydroperoxide metabolism results in accumulation of these unstable intermediates, allowing for greater degradation of oxidized PUFA via Hock cleavage to 4-HNE and 4-ONE [20]. Interestingly, SOD2 levels were increased in EWAT of *ob/ob* mice suggesting that superoxide anion is converted more efficiently to hydrogen peroxide. In conjunction with decreases in the capacity to metabolize hydrogen peroxide, this accumulation may contribute to increased production of hydroxyl radicals and accumulation of lipid hydroperoxides. These results provide the basis for the model that over nutrition leads to metabolic dysregulation in EWAT resulting in decreased metabolic capacity of both hydrogen peroxide and lipid aldehydes resulting in accumulation of oxidative stress products.

In contrast to EWAT, high fat fed C57Bl/6J and *ob/ob* mouse SAT exhibited only a trend towards decreased expression of Prdx3, and SOD2. Consistent with previous reports, GSTA4 levels were decreased significantly [4, 11]. Interestingly, ALDH2 expression was decreased in EWAT and SAT of ob/ob mice, which is consistent with the increases in lipid aldehydes observed in EWAT, but not in SAT. The antioxidant gene expression profile in EWAT is consistent with increased lipid peroxidation, but does not adequately explain the decreases in lipid aldehydes observed in SAT or the dramatic differences between the two tissues. However, metabolism of products of oxidative stress is complex, with multiple classes of both phase I and phase II enzymes contributing to biotransformation of a variety of classes of molecules. Alternatively, the mechanisms by which subcutaneous adipose tissue responds differently to high fat diet than visceral adipose tissue may be linked to decreased inflammatory macrophages present in subcutaneous fat relative to visceral depots [64, 65]. Interestingly, levels of 4-HNE and 4-ONE along with protein carbonylation were decreased in subcutaneous adipose tissue. Many reports suggest that increased visceral adipose tissue correlates more strongly with metabolic disease than subcutaneous adipose tissue [54, 55, 56]. Decreased levels of 4-HNE and 4-ONE suggest that subcutaneous tissue may undergo a robust antioxidant response to high fat feeding, resulting in decreased oxidative stress.

Obesity is associated with a chronic low-grade inflammatory state characterized by macrophage infiltration into adipose tissue [66]. Macrophage infiltration of visceral adipose depots is greater than in subcutaneous depots and may drive the metabolic dysfunction associated with obesity [65]. These macrophages produce and secrete large amounts of proinflammatory cytokines, such as tumor necrosis factor α (TNFα) [67]. Treatment of 3T3-L1 adipocytes with TNFα resulted in decreased expression of GSTA4, GPx4, and Prdx3. In contrast, SOD2 expression increased dramatically. These changes are consistent with increased production, and decreased metabolism, of H_2O_2, providing substrate for production of hydroxyl radical and subsequent lipid peroxidation. These results provide evidence that inflammation may be responsible for propagation of oxidative stress in EWAT exposed to activated macrophages [65]. Moreover, since SAT is not infiltrated with macrophages to the same extent as is EWAT, oxidative stress has been suggested to be less critical for SAT depots [65]. Moreover, several antioxidant genes such as Prdx3 and ALDH2

were not down regulated in SAT in response to high fat feeding suggesting that the decreased aldehydes and protein carbonylation may be due to antioxidant enzyme action. Further characterization of free radicals and other reactive oxygen species in conjunction with inflammatory signaling pathways may provide further evidence regarding the differences in disposition of EWAT and SAT in response to over nutrition.

Acknowledgments

The authors thank the Minnesota Supercomputing Institute for computational and data storage support and the Minnesota Center for Mass Spectrometry and Proteomics for instrument usage. This work was funded by NIH DK084669 DAB and F32 DK091004 to EKL and the Minnesota Obesity Center (NIH DK050456).

ABBREVIATIONS

EWAT	epididymal white adipose tissue
SAT	subcutaneous white adipose tissue
4-HNE	*trans*-4-hydroxy-2-nonenal
4-ONE	*trans*-4-oxo-2-nonenal
4-HNE-d_3	trans-4-hydroxy-2-nonenal-9,9,9-d_3
4-O NE-d_3	trans-4-oxo-2-nonenal-9,9,9-d_3
MDA	malondialdehyde
4-HHE	trans-4-hydroxy-2-hexenal
GS-HHE	glutathionyl trans-4-hydroxy-2-hexenal
PUFA	polyunsaturated fatty acids
GSTA4	glutathione-S-transferase A4
Gpx4	glutathione peroxidase 4
GPx3	glutathione peroxidase 3
Prdx3	peroxiredoxin 3
SOD2	manganese superoxide dismutase
ALDH2	aldehyde dehydrogenase 2
AOA	aminooxyacetic acid
BHT	butylated hydroxytoluene
DTPA	Diethylenetriaminepentaacetic acid
LLOQ	lower limit of quantitation
RSD	relative standard deviation
LF	low fat diet
HF	high fat diet

REFERENCES

[1]. Ferroni P, Basili S, Falco A, Davi G. Inflammation, insulin resistance, and obesity. Curr Atheroscler Rep. 2004; 6:424–431. [PubMed: 15485587]

[2]. Furukawa S, Fujita T, Shimabukuro M, Iwaki M, Yamada Y, Nakajima Y, Nakayama O, Makishima M, Matsuda M, Shimomura I. Increased oxidative stress in obesity and its impact on metabolic syndrome. J Clin Invest. 2004; 114:1752–1761. [PubMed: 15599400]

[3]. Sankhla M, Sharma TK, Mathur K, Rathor JS, Butolia V, Gadhok AK, Vardey SK, Sinha M, Kaushik GG. Relationship of oxidative stress with obesity and its role in obesity induced metabolic syndrome. Clin Lab. 2012; 58:385–392. [PubMed: 22783566]

[4]. Curtis JM, Grimsrud PA, Wright WS, Xu X, Foncea RE, Graham DW, Brestoff JR, Wiczer BM, Ilkayeva O, Cianflone K, Muoio DE, Arriaga EA, Bernlohr DA. Downregulation of adipose glutathione S-transferase A4 leads to increased protein carbonylation, oxidative stress, and mitochondrial dysfunction. Diabetes. 2010; 59:1132–1142. [PubMed: 20150287]

[5]. Curtis JM, Hahn WS, Long EK, Burrill JS, Arriaga EA, Bernlohr DA. Protein carbonylation and metabolic control systems. Trends Endocrinol Metab. 2012; 23:399–406. [PubMed: 22742812]

[6]. Singh SP, Niemczyk M, Saini D, Awasthi YC, Zimniak L, Zimniak P. Role of the electrophilic lipid peroxidation product 4-hydroxynonenal in the development and maintenance of obesity in mice. Biochemistry. 2008; 47:3900–3911. [PubMed: 18311940]

[7]. Zimniak P. 4-Hydroxynonenal and fat storage: A paradoxical pro-obesity mechanism? Cell Cycle. 2010; 9:3393–3394. [PubMed: 20855977]

[8]. Oh DY, Morinaga H, Talukdar S, Bae EJ, Olefsky JM. Increased macrophage migration into adipose tissue in obese mice. Diabetes. 2012; 61:346–354. [PubMed: 22190646]

[9]. Yuzefovych LV, Musiyenko SI, Wilson GL, Rachek LI. Mitochondrial DNA damage and dysfunction, and oxidative stress are associated with endoplasmic reticulum stress, protein degradation and apoptosis in high fat diet-induced insulin resistance mice. PloS one. 2013; 8:e54059. [PubMed: 23342074]

[10]. Curtis JM, Hahn WS, Stone MD, Inda JJ, Droullard DJ, Kuzmicic JP, Donoghue MA, Long EK, Armien AG, Lavandero S, Arriaga E, Griffin TJ, Bernlohr DA. Protein carbonylation and adipocyte mitochondria function. J Biol Chem. 2012

[11]. Grimsrud PA, Picklo M. J., Sr. Griffin TJ, Bernlohr DA. Carbonylation of adipose proteins in obesity and insulin resistance: identification of adipocyte fatty acid-binding protein as a cellular target of 4-hydroxynonenal. Mol Cell Proteomics. 2007; 6:624–637. [PubMed: 17205980]

[12]. Grimsrud PA, Xie H, Griffin TJ, Bernlohr DA. Oxidative stress and covalent modification of protein with bioactive aldehydes. J Biol Chem. 2008; 283:21837–21841. [PubMed: 18445586]

[13]. Schaur RJ. Basic aspects of the biochemical reactivity of 4-hydroxynonenal. Mol Aspects Med. 2003; 24:149–159. [PubMed: 12892992]

[14]. Bennaars-Eiden A, Higgins L, Hertzel AV, Kapphahn RJ, Ferrington DA, Bernlohr DA. Covalent modification of epithelial fatty acid-binding protein by 4-hydroxynonenal in vitro and in vivo. Evidence for a role in antioxidant biology. J Biol Chem. 2002; 277:50693–50702. [PubMed: 12386159]

[15]. Esterbauer H, Schaur RJ, Zollner H. Chemistry and biochemistry of 4-hydroxynonenal, malonaldehyde and related aldehydes. Free Radic Biol Med. 1991; 11:81–128. [PubMed: 1937131]

[16]. Stewart BJ, Doorn JA, Petersen DR. Residue-specific adduction of tubulin by 4-hydroxynonenal and 4-oxononenal causes cross-linking and inhibits polymerization. Chem Res Toxicol. 2007; 20:1111–1119. [PubMed: 17630713]

[17]. Tsuchiya Y, Yamaguchi M, Chikuma T, Hojo H. Degradation of glyceraldehyde-3-phosphate dehydrogenase triggered by 4-hydroxy-2-nonenal and 4-hydroxy-2-hexenal. Arch Biochem Biophys. 2005; 438:217–222. [PubMed: 15907785]

[18]. Picklo MJ, Azenkeng A, Hoffmann MR. Trans-4-oxo-2-nonenal potently alters mitochondrial function. Free Radic Biol Med. 2011; 50:400–407. [PubMed: 21092757]

[19]. Picklo MJ Sr. Montine TJ. Mitochondrial effects of lipid-derived neurotoxins. J Alzheimers Dis. 2007; 12:185–193. [PubMed: 17917163]

[20]. Gardner HW. Oxygen radical chemistry of polyunsaturated fatty acids. Free Radic Biol Med. 1989; 7:65–86. [PubMed: 2666279]

[21]. Doorn JA, Petersen DR. Covalent modification of amino acid nucleophiles by the lipid peroxidation products 4-hydroxy-2-nonenal and 4-oxo-2-nonenal. Chem Res Toxicol. 2002; 15:1445–1450. [PubMed: 12437335]

[22]. Doorn JA, Petersen DR. Covalent adduction of nucleophilic amino acids by 4-hydroxynonenal and 4-oxononenal. Chem Biol Interact. 2003; 143–144:93–100.

[23]. Uchida K. A lipid-derived endogenous inducer of COX-2: a bridge between inflammation and oxidative stress. Mol Cells. 2008; 25:347–351. [PubMed: 18483467]

[24]. Frohnert BI, Sinaiko AR, Serrot FJ, Foncea RE, Moran A, Ikramuddin S, Choudry U, Bernlohr DA. Increased adipose protein carbonylation in human obesity. Obesity (Silver Spring). 2011; 19:1735–1741. [PubMed: 21593812]

[25]. Long EK, Smoliakova I, Honzatko A, Picklo MJ Sr. Structural characterization of alpha,beta-unsaturated aldehydes by GC/MS is dependent upon ionization method. Lipids. 2008; 43:765–774. [PubMed: 18592287]

[26]. Lee SH, Blair IA. Characterization of 4-oxo-2-nonenal as a novel product of lipid peroxidation. Chem Res Toxicol. 2000; 13:698–702. [PubMed: 10956056]

[27]. Choudhary S, Xiao T, Vergara LA, Srivastava S, Nees D, Piatigorsky J, Ansari NH. Role of aldehyde dehydrogenase isozymes in the defense of rat lens and human lens epithelial cells against oxidative stress. Invest Ophthalmol Vis Sci. 2005; 46:259–267. [PubMed: 15623782]

[28]. Liu G, Feinstein SI, Wang Y, Dodia C, Fisher D, Yu K, Ho YS, Fisher AB. Comparison of glutathione peroxidase 1 and peroxiredoxin 6 in protection against oxidative stress in the mouse lung. Free Radic Biol Med. 2010; 49:1172–1181. [PubMed: 20627125]

[29]. Sacks HS, Fain JN, Cheema P, Bahouth SW, Garrett E, Wolf RY, Wolford D, Samaha J. Depot-specific overexpression of proinflammatory, redox, endothelial cell, and angiogenic genes in epicardial fat adjacent to severe stable coronary atherosclerosis. Metabolic syndrome and related disorders. 2011; 9:433–439. [PubMed: 21679057]

[30]. Hjelle JJ, Petersen DR. Hepatic aldehyde dehydrogenases and lipid peroxidation. Pharmacol Biochem Behav. 1983; 18(Suppl 1):155–160. [PubMed: 6634832]

[31]. Student AK, Hsu RY, Lane MD. Induction of fatty acid synthetase synthesis in differentiating 3T3-L1 preadipocytes. J Biol Chem. 1980; 255:4745–4750. [PubMed: 7372608]

[32]. Guidance for Industry, Bioanalytical Method Validation. US Department of Health and Human Services, Food and Drug Administration, Center for Drug Evaluation and Research (CDER), Center for Veterinary Medicine (CVM). 2001.

[33]. Starkenmann C. Analysis of a model reaction system containing cysteine and (E)-2-methyl-2-butenal, (E)-2-hexenal, or mesityl oxide. J Agric Food Chem. 2003; 51:7146–7155. [PubMed: 14611186]

[34]. Tanti JF, Ceppo F, Jager J, Berthou F. Implication of inflammatory signaling pathways in obesity-induced insulin resistance. Frontiers in endocrinology. 2012; 3:181. [PubMed: 23316186]

[35]. Wang X, Cheng M, Zhao M, Ge A, Guo F, Zhang M, Yang Y, Liu L, Yang N. Differential effects of high-fat-diet rich in lard oil or soybean oil on osteopontin expression and inflammation of adipose tissue in diet-induced obese rats. European journal of nutrition. 2012

[36]. Rossi MA, Fidale F, Di Mauro C, Esterbauer H, Dianzani MU. Effect of 4-hydroxy-2,3-trans-nonenal and related aldehydes on phospholipase C activity of rat neutrophils. Int J Tissue React. 1993; 15:201–205. [PubMed: 8077089]

[37]. Selley ML. Determination of the lipid peroxidation product (E)-4-hydroxy-2-nonenal in clinical samples by gas chromatography--negative-ion chemical ionisation mass spectrometry of the O-pentafluorobenzyl oxime. J Chromatogr B Biomed Sci Appl. 1997; 691:263–268. [PubMed: 9174261]

[38]. Selley ML, Bartlett MR, McGuiness JA, Hapel AJ, Ardlie NG. Determination of the lipid peroxidation product trans-4-hydroxy-2-nonenal in biological samples by high-performance liquid chromatography and combined capillary column gas chromatography-negative-ion chemical ionisation mass spectrometry. J Chromatogr. 1989; 488:329–340. [PubMed: 2745626]

[39]. Awasthi YC, Sharma R, Cheng JZ, Yang Y, Sharma A, Singhal SS, Awasthi S. Role of 4-hydroxynonenal in stress-mediated apoptosis signaling. Mol Aspects Med. 2003; 24:219–230. [PubMed: 12893000]

[40]. Bradley MA, Markesbery WR, Lovell MA. Increased levels of 4-hydroxynonenal and acrolein in the brain in preclinical Alzheimer disease. Free Radic Biol Med. 48:1570–1576. [PubMed: 20171275]

[41]. Eckl PM, Ortner A, Esterbauer H. Genotoxic properties of 4-hydroxyalkenals and analogous aldehydes. Mutat Res. 1993; 290:183–192. [PubMed: 7694109]

[42]. Kumagai T, Matsukawa N, Kaneko Y, Kusumi Y, Mitsumata M, Uchida K. A lipid peroxidation-derived inflammatory mediator: identification of 4-hydroxy-2-nonenal as a potential inducer of cyclooxygenase-2 in macrophages. J Biol Chem. 2004; 279:48389–48396. [PubMed: 15355999]

[43]. Kumagai T, Nakamura Y, Osawa T, Uchida K. Role of p38 mitogen-activated protein kinase in the 4-hydroxy-2-nonenal-induced cyclooxygenase-2 expression. Arch Biochem Biophys. 2002; 397:240–245. [PubMed: 11795877]

[44]. Minekura H, Kumagai T, Kawamoto Y, Nara F, Uchida K. 4-Hydroxy-2-nonenal is a powerful endogenous inhibitor of endothelial response. Biochem Biophys Res Commun. 2001; 282:557–561. [PubMed: 11401496]

[45]. Poli G, Biasi F, Leonarduzzi G. 4-Hydroxynonenal-protein adducts: A reliable biomarker of lipid oxidation in liver diseases. Mol Aspects Med. 2008; 29:67–71. [PubMed: 18158180]

[46]. Siems WG, Grune T, Esterbauer H. 4-Hydroxynonenal formation during ischemia and reperfusion of rat small intestine. Life Sci. 1995; 57:785–789. [PubMed: 7637552]

[47]. Toyokuni S, Yamada S, Kashima M, Ihara Y, Yamada Y, Tanaka T, Hiai H, Seino Y, Uchida K. Serum 4-hydroxy-2-nonenal-modified albumin is elevated in patients with type 2 diabetes mellitus. Antioxid Redox Signal. 2000; 2:681–685. [PubMed: 11213473]

[48]. Uchida K, Stadtman ER. Covalent attachment of 4-hydroxynonenal to glyceraldehyde-3-phosphate dehydrogenase. A possible involvement of intra- and intermolecular cross-linking reaction. J Biol Chem. 1993; 268:6388–6393. [PubMed: 8454610]

[49]. Williams TI, Lynn BC, Markesbery WR, Lovell MA. Increased levels of 4-hydroxynonenal and acrolein, neurotoxic markers of lipid peroxidation, in the brain in Mild Cognitive Impairment and early Alzheimer's disease. Neurobiol Aging. 2006; 27:1094–1099. [PubMed: 15993986]

[50]. Liu Y, Longmore RB. Dietary sandalwood seed oil modifies fatty acid composition of mouse adipose tissue, brain, and liver. Lipids. 1997; 32:965–969. [PubMed: 9307938]

[51]. Tallman DL, Taylor CG. Effects of dietary fat and zinc on adiposity, serum leptin and adipose fatty acid composition in C57BL/6J mice. J Nutr Biochem. 2003; 14:17–23. [PubMed: 12559473]

[52]. Gerard-Monnier D, Erdelmeier I, Regnard K, Moze-Henry N, Yadan JC, Chaudiere J. Reactions of 1-methyl-2-phenylindole with malondialdehyde and 4-hydroxyalkenals. Analytical applications to a colorimetric assay of lipid peroxidation. Chem Res Toxicol. 1998; 11:1176–1183. [PubMed: 9778314]

[53]. Drechsel DA, Patel M. Differential contribution of the mitochondrial respiratory chain complexes to reactive oxygen species production by redox cycling agents implicated in parkinsonism. Toxicol Sci. 2009; 112:427–434. [PubMed: 19767442]

[54]. Kyrou I, Chrousos GP, Tsigos C. Stress, visceral obesity, and metabolic complications. Ann N Y Acad Sci. 2006; 1083:77–110. [PubMed: 17148735]

[55]. Matsuzawa Y, Shimomura I, Nakamura T, Keno Y, Kotani K, Tokunaga K. Pathophysiology and pathogenesis of visceral fat obesity. Obes Res. 1995; 3(Suppl 2):187S–194S. [PubMed: 8581775]

[56]. Coate KC, Huggins KW. Consumption of a high glycemic index diet increases abdominal adiposity but does not influence adipose tissue pro-oxidant and antioxidant gene expression in C57BL/6 mice. Nutr Res. 30:141–150. [PubMed: 20227000]

[57]. Huh JY, Kim Y, Jeong J, Park J, Kim I, Huh KH, Kim YS, Woo HA, Rhee SG, Lee KJ, Ha H. Peroxiredoxin 3 is a key molecule regulating adipocyte oxidative stress, mitochondrial biogenesis, and adipokine expression. Antioxid Redox Signal. 2011; 16:229–243. [PubMed: 21902452]

[58]. Lee YS, Kim AY, Choi JW, Kim M, Yasue S, Son HJ, Masuzaki H, Park KS, Kim JB. Dysregulation of adipose glutathione peroxidase 3 in obesity contributes to local and systemic oxidative stress. Mol Endocrinol. 2008; 22:2176–2189. [PubMed: 18562625]

[59]. Balogh LM, Atkins WM. Interactions of glutathione transferases with 4-hydroxynonenal. Drug metabolism reviews. 2011; 43:165–178. [PubMed: 21401344]

[60]. Balogh LM, Le Trong I, Kripps KA, Shireman LM, Stenkamp RE, Zhang W, Mannervik B, Atkins WM. Substrate specificity combined with stereopromiscuity in glutathione transferase A4-4-dependent metabolism of 4-hydroxynonenal. Biochemistry. 2010; 49:1541–1548. [PubMed: 20085333]

[61]. Vatsyayan R, Lelsani PC, Chaudhary P, Kumar S, Awasthi S, Awasthi YC. The expression and function of vascular endothelial growth factor in retinal pigment epithelial (RPE) cells is regulated by 4-hydroxynonenal (HNE) and glutathione S-transferaseA4-4. Biochem Biophys Res Commun. 2012; 417:346–351. [PubMed: 22155253]

[62]. Muthukumar K, Rajakumar S, Sarkar MN, Nachiappan V. Glutathione peroxidase3 of Saccharomyces cerevisiae protects phospholipids during cadmium-induced oxidative stress. Antonie van Leeuwenhoek. 2011; 99:761–771. [PubMed: 21229313]

[63]. Nagy P, Karton A, Betz A, Peskin AV, Pace P, O'Reilly RJ, Hampton MB, Radom L, Winterbourn CC. Model for the exceptional reactivity of peroxiredoxins 2 and 3 with hydrogen peroxide: a kinetic and computational study. J Biol Chem. 2011; 286:18048–18055. [PubMed: 21385867]

[64]. Korsic M, Gotovac K, Nikolac M, Dusek T, Skegro M, Muck-Seler D, Borovecki F, Pivac N. Gene expression in visceral and subcutaneous adipose tissue in overweight women. Frontiers in bioscience (Elite edition). 2012; 4:2834–2844. [PubMed: 22652682]

[65]. Alvehus M, Buren J, Sjostrom M, Goedecke J, Olsson T. The human visceral fat depot has a unique inflammatory profile. Obesity (Silver Spring). 2010; 18:879–883. [PubMed: 20186138]

[66]. Olefsky JM, Glass CK. Macrophages, inflammation, and insulin resistance. Annual review of physiology. 2010; 72:219–246.

[67]. Tzanavari T, Giannogonas P, Karalis KP. TNF-alpha and obesity. Current directions in autoimmunity. 2010; 11:145–156. [PubMed: 20173393]

Highlights

- Over nutrition increases lipid peroxidation in epididymal adipose tissue.
- Over nutrition decreases lipid peroxidation in subcutaneous adipose tissue.
- *Trans*-4-oxo-2-nonenal is a major product of lipid peroxidation in adipose tissue.
- Over nutrition decreases antioxidant genes in visceral, not subcutaneous adipose.

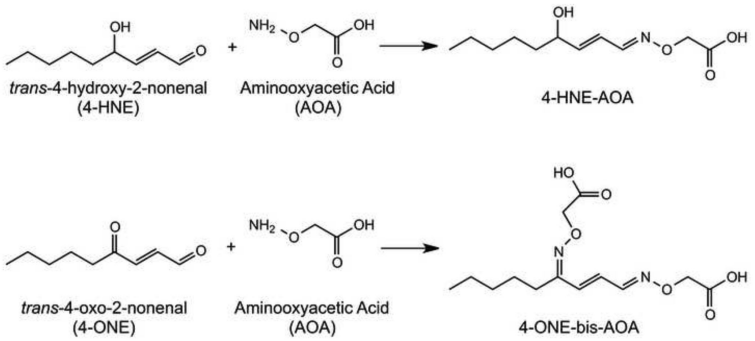

Figure 1. Derivatization of Aldehydes With Aminooxyacetic Acid

Schematic representation of the reaction between aminooxyacetic acid and either 4-HNE or 4-ONE resulting in oxime formation.

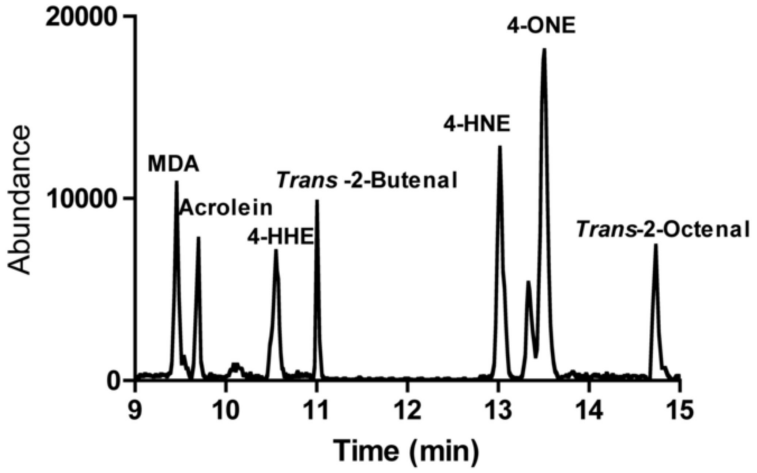

Figure 2. Standard Aldehyde Chromatogram

A mixture of synthetic aldehydes was derivatized using aminooxyacetic acid and separated via LCMS/MS as described in Materials and Methods. The resolved lipids were analyzed using a AB/Sciex API 4000Qtrap mass spectrometer.

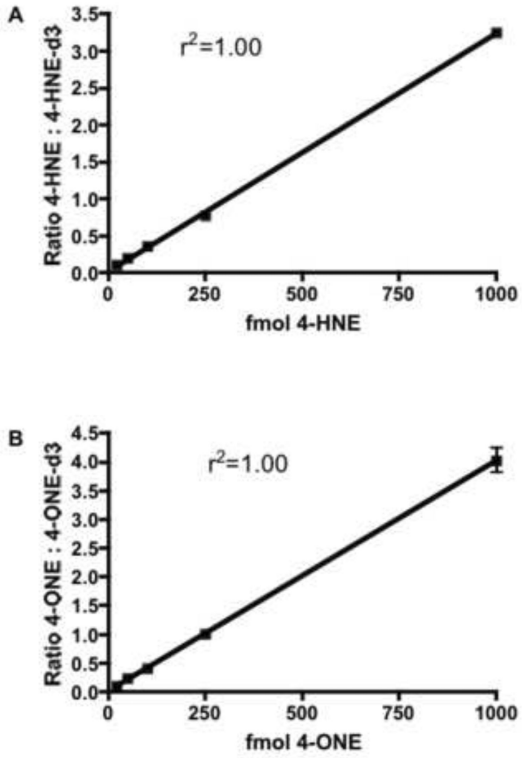

Figure 3. Calibration Curves for AOA-derivatized 4-HNE and 4-ONE

The indicated amounts of 4-HNE (A) and 4-ONE (B) were incubated with 50 mg adipose tissue homogenate and derivatized with aminooxyacetic acid. 4-HNE and 4-ONE oxime derivatives were extracted, separated and quantified by stable isotope dilution using 4-HNE-d_3 and 4-ONE-d_3, respectively. Linearity was assessed using linear regression analysis.

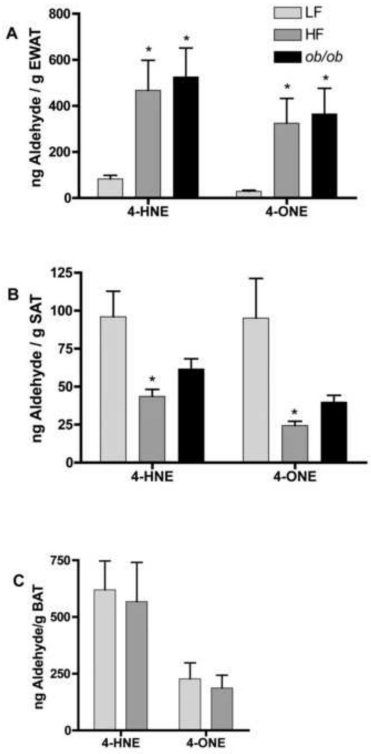

Figure 4. Adipose Tissue Levels of 4-HNE and 4-ONE

Adipose tissue from C57Bl/6J mice fed either chow (LF) or high fat (HF) diet for 9 weeks post-weaning or *ob*/*ob* leptin deficient mice was harvested and analyzed for 4-HNE and 4-ONE levels. (A) epididymal adipose tissue (n=6 for chow fed mice, n=10 for high fat fed mice, n=6 for *ob*/*ob* mice), (B) subcutaneous adipose tissue (n=7 for chow and high fat fed mice, n=6 for *ob*/*ob* mice), (C) and brown adipose tissue (n=7 for chow and high fat fed mice). *Denotes statistically significant difference between control and experimental groups with $p<0.05$ as determined by an unpaired student's t-test.

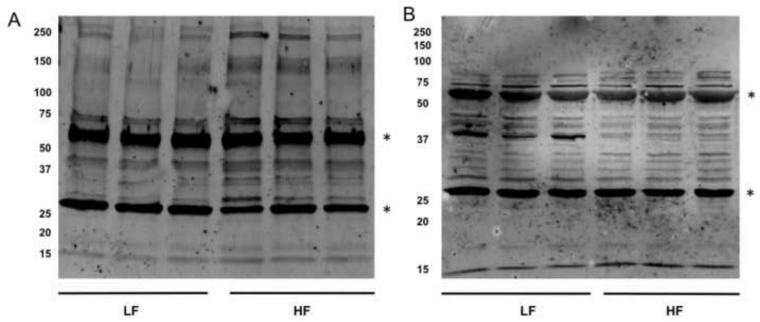

Figure 5. 4-HNE and 4-ONE Protein Adducts in Visceral and Subcutaneous Adipose Tissue

20 μg of total protein from EWAT (A) or SAT (C) was separated by SDS-PAGE, transferred to PVDF membranes and treated with an antibody specific for 4-HNE/4-ONE Michael adducts. The heavily carbonylated bands at ~ 30 kDa and ~ 67 kDa (*) represent serum proteins and are not included in the data analysis. Quantified bands for EWAT (B) and SAT (D) were normalized to actin and represented as bar graphs. *Denotes a statistically significant difference ($p<0.05$) between low fat and high fat-fed groups.

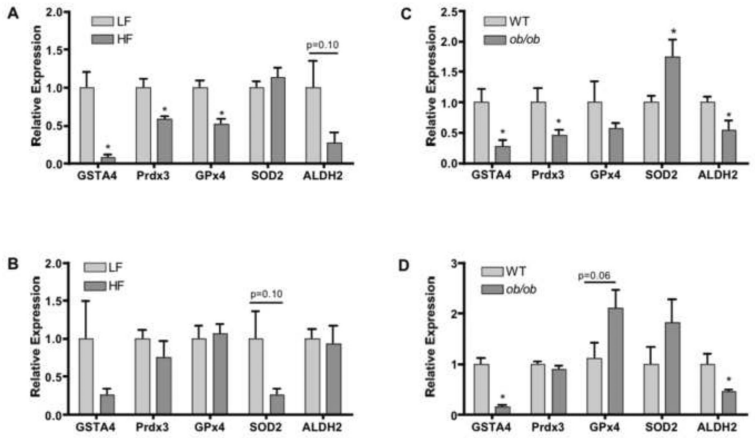

Figure 6. Expression of Genes Linked to Antioxidant Biology in Adipose Tissue

Relative expression of GSTA4, Prdx3, GPx4, SOD2, and ALDH2 in EWAT (A) and SAT (B) of high fat fed (HF) and chow fed (LF) C57Bl/6J mice measured by qRT-PCR. Relative expression of GSTA4, Prdx3, GPx4, SOD2, and ALDH2 in EWAT (C) and SAT (D) of wild-type C57Bl/6J and *ob*/*ob* mice measured by qRT-PCR. *Denotes a statistically significant difference ($p<0.05$) between control and experimental groups for each gene analyzed.

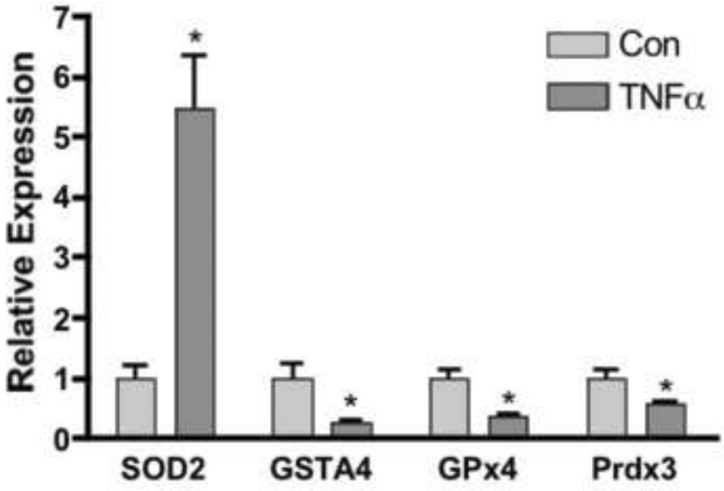

Figure 7. Regulation of Gene Expression in 3T3-L1 Adipocytes by TNFα

3T3-L1 day 8 adipocytes were incubated for 24 h with 1 nmol/L TNFα and harvested for analysis of SOD2 GSTA4, Gpx4, Prdx3, expression via qRT-PCR. *Denotes a significantly significant difference ($p<0.05$) between control and treatment groups for each gene analyzed.

Table 1

Multiple Reaction Monitoring Conditions

Analyte	MRM 1 (m/z)	MRM 2 (m/z)	MRM 3 (m/z)
4-HNE	228.1 / 75.1	228.1 / 99.1	228.1 / 136.3
4-ONE	299.3 / 75.2	299.3 / 149.3	299.3 / 225.1
4-HHE	186.3 / 75.2	186.3 / 94.2	186.3 / 110.1
Malondialdehyde	217.0 / 75.2	217.0 / 67.2	217.0 / 141.2
Trans-2-Octenal	198.0 / 75.2	198.0 / 122.0	198.0 / 124.1
Trans-2-Butenal	142.1 / 75.2	142.1 / 66.3	142.1 / 68.1
Acrolein	128.1 / 75.2	128.1 / 52.2	128.1 / 54.2
4-HNE-d3	231.1 / 75.2	231.1 / 102.1	231.1 / 139.3
4-ONE-d3	302.3 / 75.2	302.3 / 152.3	302.3 / 228.1

Table 2

Intra-day Precision (%RSD)

fmol on column	4-HNE	4-ONE
10	---	---
20	8.56	2.41
50	10.34	9.45
100	6.77	4.75
250	2.97	7.58
1000	9.70	5.08

Table 3

Accuracy (% Authentic Standard)

fmol on column	4-HNE	4-ONE
20	65	73
50	110	118
250	99	106
1000	94	111

Table 4

qRT-PCR Primer Sequence

Target	Forward and Reverse Primers
SOD2	Fw: 5'-GCGAGGAGAAGTACCACGAG
	Re: 5'-GCTTGATAGCCTCCAGCAA
Gpx4	Fw: 5'-GCTGTGCGCGCTCCAT
	Re: 5'-CCATGTGCCCGTCGATGT
Prdx3	Fw: 5'-GCAGCTGCGGGAAGGTTGCT
	Re: 5'-TGCTGGGTGACAGCAGGGGT
GSTA4	Fw: 5'-CGATGGGATGATGCTGACACA
	Re: 5'-CACTGGGAAGTAACGGGTTTTAGC
TFIIE	Fw: 5'-CAAGGCTTTAGGGGACCAGATAC
	Re: 5'-CATCCATTGACTCCACAGTGACAC
ALDH2	Fw: 5'-TTTATCCAGCCCACCGTGTTC
	Re: 5'-CAAGCCCATACTTAGAATCATTGG